Numerical simulation of microchannel double-pipe heat exchanger with ribs

Cite as: AIP Conference Proceedings **2437**, 020165 (2022); https://doi.org/10.1063/5.0093220
Published Online: 17 August 2022

J. K. Adebayo, S. O. Oyedepo, M. O. Petinrin, et al.

Numerical Simulation of Microchannel Double-Pipe Heat Exchanger with Ribs

J. K. Adebayo[1,a)], S. O. Oyedepo[2], M. O. Petinrin[1], A. A. Dare[1], C. N. Nwaokocha[3], A. T. Layeni[3], O. S. I. Fayomi[4], J. O. Dirisu[2] and O. KIlanko[2]

[1]*Department of Mechanical Engineering, University of Ibadan, Ibadan, Oyo State, Nigeria*
[2]*Department of Mechanical Engineering, Covenant University, Ota, Ogun State, Nigeria*
[3]*Mechanical Engineering Department, Olabisi Onabanjo University, College of Engineering and Environmental Studies, Ibogun Campus, Ifo, Ogun State, Nigeria.*
[4]*Department of Mechanical and Biomedical Engineering, Bells University of Technology, Ota, Ogun State, Nigeria*
[a)] Corresponding author:jacobkadebayo@gmail.com

Abstract: This study numerically investigates a double pipe heat exchanger with triangle and rectangle rib. The simulation is performed using ANSYS package, considering turbulent flow and k-e turbulence model. The working fluid is water in both tube and annulus and the flow arrangement is counter flow. The results show that, the heat transfer of triangle rib and rectangle rib are higher than that of normal DPHE and as the Reynolds number is increasing heat transfer, coefficient of heat transfers and Nusselt number are also increasing. Triangle rib has thermal performance factor of 0.9786 at Re of 40000 and rectangle rib has 1.0290 at Re of 30000. Furthermore, total heat transfer of DPHE with triangle rib is 33% better than normal DPHE at Re of 40000 and that of rectangle rib is 45%better at Re of 40000.

Key words: Rectangular rib, triangular rib, ANSYS fluent and Thermal Performance.

INTRODUCTION

Energy is core to the sustenance of man, the more the activities of man, the more the demand and consumption of energy [7].

Heat exchanger (HE) is a common industrial equipment that can move heat energy from hot region to cold region without the two medium mix together [35]. This thermal equipment consume energy which is a challenge [32]. Efficient heat exchanger is achieved by which is only possible through active and passive method [6]. Modification of HE geometry is key to improve its performance, efficient and energy conservation [5].

Double pipe heat exchanger (DPHE) frequently used in refinery and other large chemical process industries because of its suit high pressure application [23]. Counter flow Double pipe heat exchanger (CDPHE) is consist of two concentric circle and it's widely used in industry because it is easily maintaining, occupy small space, low-cost and easy to manufacture [29]. The flow of the streams is in opposite direction [27] [14].

Different method has been employed and numerous ideals have been introduced in other to improve the performance and efficient and effectiveness of DPHE.

DPHE is used in chemical, food, gas industries [24], heating or cooling fluid and evaporation or condensation of vapour or stream [22] and thermodynamic vent system (TVS) [18]. The result of these could be to remove heat or regain it, purify liquid or separate it [3].

Zare experiment both counter flow (CF) and parallel flow (PF) and find out that CF transfer heat more efficiently than PF at the same flow rate. He also discovered that in a way, DPHE control environmental pollution [35]. Sajid's work also confirmed it and noted that Straight tube CDHE's effectiveness is 7-10% more than helical coil parallel flow HE. Using outward helically corrugated tube with inner diameter 20mm and shell diameter 38mm are dimension

Technologies and Materials for Renewable Energy, Environment and Sustainability
AIP Conf. Proc. 2437, 020165-1–020165-11; https://doi.org/10.1063/5.0093220
Published by AIP Publishing. 978-0-7354-4372-3/$30.00

which highest HT coefficient, and a low pressure drop [34]. However, corrugated tube [4] and baffles attached to annulus [10], [26], split longitudinal fins (SLF) [9] on the annulus side, helical fins [13] or fins generally [15 and [20] increase HTP and reduce pressure compared to the simple d. Also in way buoyancy effect is significant in the pseudo-critical region especially at different pressures.

Generally, Khan discovered that the HE advances with the Re number [25] and reduces when Da number increases. In case of porous medium [14] Da numbers, Nusselt number and Re number [8] have positive effective on HE effectiveness [30]. Perforated self-rotated twist tape experimentally showed better thermal performance [36].

Nitrogen-doped graphene (NDG) [11] and Fe_3O_4 [21] [17] [16] [12] nanofluids enhance convective heat transfer coefficient compare to water. TiO_2 increase the Reynolds number and Nusselt number. Al_2O_3-TiO_2 hybrid nano fluids boost exergy efficiency [19]. This experimental result so that most nanofluids have a higher Nusselt number compared to distilled water [31]. Therefore, when high Re is used with nanofluid more power is need but if the Re is low then pressure drop will be low also power needed [22].

Experiment and CFD simulation of DPHE using fins at different angle (0^0, 5^0, 10^0, 15^0, 20^0, 25^0) was carried out. It was discovered that heat transfer rate increase from 1494.75 W to1920.05 W and overall heat transfer coefficient (734.58 W/m^2 ^{0}C to 1570.46 W/m^{20}C as the fins angle increase from 0^0 to 20^0 but beyond this angle both heat HT rate and overall heat transfer coefficient decrease [23]. Circular fin of height 2mm to 3mm also increases HT by 36% and 30% for any fluid [29]. Up to 22.3% increase in heat transfer were discovered in a DPHE when the tube was made to rotate, varied from 0 to 500rpm and eccentricity 0 t0 40mm [2]. Vibration of the tube also improve heat transfer [28].

PHYSICAL MODELS

The purpose of this numerical simulation is to check the effect of rectangle and triangle on the tube of DPHE. The introduction ribs to DPHE affects the pressure distribution in the shell (annulus) which affect heat energy movement within the device [29 – 35]. The configurations of rectangle rib and triangle rib in DPHE are shown in FIGURE 1 below. The effect geometric on thermal performance other fluid properties were numerically investigated. The details of DPHE is: the annulus inner diameter D_a = 20mm tube outer diameter D_t =10mm and DPHE length L = 200mm. The thickness (h) and length along the tube circle of tube (t) are h = 0.5mm and t = 1.85mm respectively.

Water at 20^{o}C flow on the annulus side and water at 5^{o}C flows in the tube side in opposite direction. The parameters of the modelled were kept constant throughout the simulation so that all the values of dimension new geometry are the same except the use of rectangular and triangular rib. The material of the HE parts is copper and its thermal conductivity is 120 W/mk.

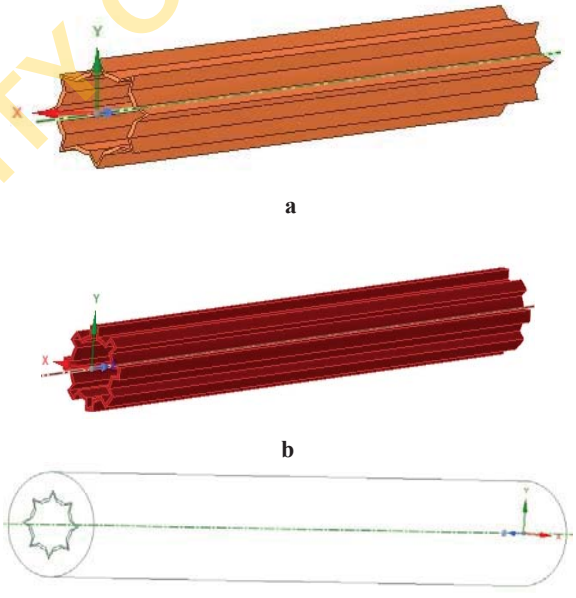

a

b

c

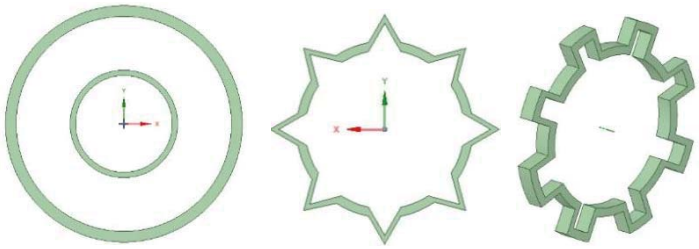

d

FIGURE 1. (a) Triangle rib of DPHE(b) Rectangle rib of DPHE (c) geometric of DPHE

(d) Schematic of considered DPHE with rectangular and triangular rib on the tube

Mathematical Model

The working fluid is water with constant physical, chemical and thermodynamic properties. The fluid flow is turbulent and is considered steady-state case [10]. In line with the pre mention properties and dimension, fluid and HT equations are solved numerically considering properties of water at the specified temperature. A standard k–ε turbulent and standard wall function were used to analyze the flow [29]. The equations below were solved.

Governing Equations

Continuity equation:

$$\frac{\partial \rho u_i}{\partial x_i} = 0 \qquad (1)$$

Momentum equation:

$$\frac{\partial \partial u_i u_i}{\partial x_i} = -\frac{1}{\rho \partial}\frac{\partial p}{x_i} + \frac{\partial}{\partial x_j}\left((v + v_t)\left(\frac{\partial u_i}{\partial x_j} + \frac{\partial u_i}{\partial x_i}\right)\right), \qquad (2)$$

Energy equation:

$$\frac{\partial u_i}{\partial x_i} = \rho \frac{\partial}{\partial x_i}\left(\frac{v}{Pr} + \frac{v_i}{Pr_i}\right)\frac{\partial T}{\partial x_i} \qquad (3)$$

where ρ = fluid density; u = velocity, T = temperature and p = pressure. ν = kinematic viscosity and Pr = Prandtl number, subscript t refers to turbulent flow.

The transport equations in the standard k -e model are given below:

Turbulent kinetic energy k equation [36 – 37]:

$$\frac{\partial u_i \varepsilon}{\partial x_i} = \frac{\partial}{\partial x_i}\left(\left(v + \frac{v_t}{\sigma_k}\right)\frac{\partial k}{\partial x_i}\right) + \Gamma - \varepsilon \qquad (4)$$

Turbulent energy dissipation ε equation:

$$\frac{\partial u_i \varepsilon}{\partial x_i} = \frac{\partial}{\partial x_i}\left(\left(v + \frac{v_t}{\sigma_k}\right)\frac{\partial k}{\partial x_i}\right) + c_i \Gamma \varepsilon - c_2 \frac{\varepsilon^2}{k + \sqrt{v\varepsilon}} \qquad (5)$$

where Γ = generation of turbulence kinetic energy k due to the mean velocity gradients and is given by:

$$\text{nas}\Gamma = \overline{u_i u_j}\frac{\partial u_i}{\partial x_i} = v_{turb}\left(\frac{\partial u_i}{\partial x_j} + \frac{\partial u_j}{\partial x_i}\right)\frac{\partial u_i}{\partial x_i} \qquad (6)$$

The turbulent kinematic viscosity is:

$$v_{turb} = c_p \frac{k^2}{\varepsilon} \qquad (7)$$

The empirical constants for the realizable k e turbulence model are [10]:

$c_2 = 1.9$; $\sigma_k = 1.0$; $C_1 = \max[0.43, \mu/(\mu_t + 5)]$; $\sigma_\varepsilon = 1.9$

Required equation

$$Re = \frac{\rho u_m d}{\mu} \quad (8)$$

Fanning friction factor

$$C_f = \frac{2\tau_s}{\rho u_m^2} \quad (9)$$

Darcy friction coefficient

$$f = \frac{2\Delta p}{\frac{1}{D}\rho L u_m^2} \quad (10)$$

$$f = 0.0014 + \frac{0.125}{Re^{0.32}} \quad (11)$$

Nusselt number

$$Nu = \frac{hD_h}{k} \quad (11)$$

$$h = \frac{\ddot{q}}{T_h - T_c} \quad (12)$$

Thermal performance factor (ɳ) is calculated as:

$$\mathfrak{y} = \left({}^{Nu}/_{Nu_n}\right) \text{ and } \left({}^{f}/_{f_n}\right)^{0.33} \quad (13)$$

TABLE 1. Thermal properties of water

Water	20^0C
C_p	
Dynamic Viscosity	0.0010005Pa-s
Kinematic viscosity	0.0000010023m^2/s
Thermal conductivity	0.607
Density	998.21kg/m^3
Prandtl number	7

Domains Definitions, Grid Independent Study and Boundary Conditions

Three arrangement or configurations of DPHEs are simulated. The first is simple used for validation secondly triangle rib was attached to it and lastly rectangle rib was used to replaced triangle rib. DPHE has three computational domains for easy simulation and two domains are water (inner tube and annulus side) and one solid domain (walls). A 3D of DPHE was model, drawn with Space-claim and simulated with ANSYS considering flow inside as turbulent. The software was used to study the flow pattern in DPHE. FIGURE 2 shows XY geometry view of DPHE with triangle rib.

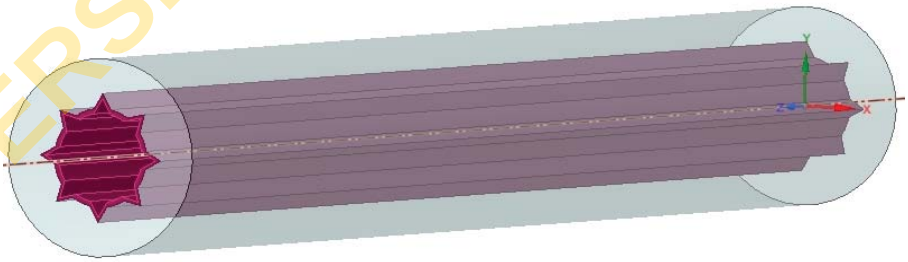

FIGURE 2. DPHE with triangle rib

The models were meshed and the method used was tetrahedron using the patch conforming algorithm as shown in FIGURE 3. The study of simulated 3D model conducted in ANSYS fluent reviewed the turbulent flow pattern of water in DPHE. FIGURE 3 shows the meshed rectangular rib of the tube of DPHE [38 – 39].

In order to have correct numerical results, the grid independent study was carried out for different elements. Meshing were done in such a way that four grids were obtained, simulated and optimized (A = 158513, B = 230073, C = 344694, and D = 598774 elements). It was found that the theoretical Nusselt number using Gnielinski–Petkhove formula and that of C are almost the same compare to other. Also looking at their rate of HT C and D are closed

compare to others. The rate of HT between C and D is small compared to other. Therefore, C was used because of time of simulation and accuracy. (see TABLE 2).

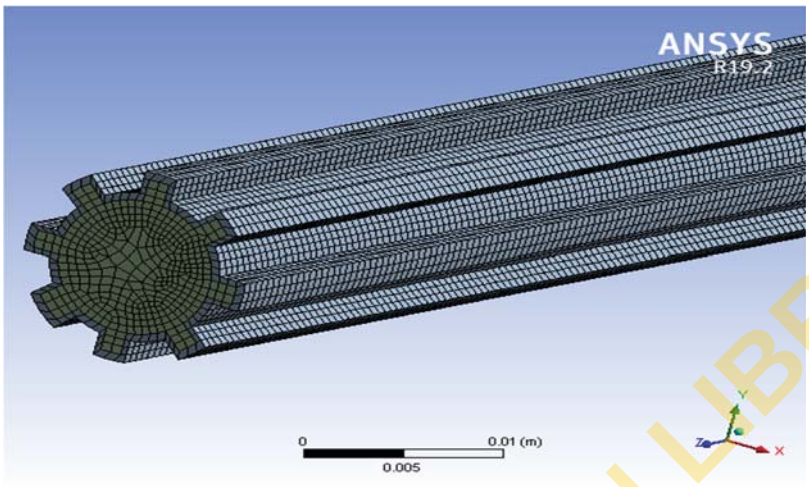

FIGURE 3. The meshing of the heat exchanger

CFD software called ANSYS Fluent was used to solve the continuity, momentum and energy equations in Cartesian coordinate system based on finite volume method. The simple standard k-e model was imposed in pressure–velocity coupling with pressure-based solver. The energy and momentum equations are discretized using second-order upwind scheme.

TABLE 2. Mesh Independence for L = 200mm Re= 5000

S/N	Elements	Nusselts Number	Percentage Different
1	158513	86.3026	28.63%
2	230073	61.596	28.63%
3	344694	46.8277	23.98
4	598774	57.922	23.69

RESULTS AND DISCUSSION

Model Validation

Numerical results were validated by simulating simple DPHE and compared the thermo-hydrodynamic characteristics of the simulated with the empirical results obtained by Gnielinski–Petkhove [29].

Flow velocity of water in shell side (hot water) was varied from 1.002 m/s ≤ U_m ≤ 2.502m/s while that of the inner tube (cold water) was always 0.5m/s below shell side. Hot water inlet temperatures were constant 20^0C and Cold water inlet temperature was constant also 5^0C.

TABLE 3 below relate the numerical results from ANSYS fluent and analytical calculations for turbulent flow of water in DPHE. The simulation is validated by putting side by side the CFD data with the analytical results outcome by Gnielinski–Petkhove [10]. $Nu = 0.023Re^{0.8}Pr^{1/3}$.

TABLE 3. Validation of Nu number and f factor

S/N	Reynolds number	Nusselt Number		Correlation Factor	
		Gnielinski	Numerical	Gnielinski	Numerical
1	20000	138	201.54	0.0067	0.0067
2	25000	165.24	244.27	0.0063	0.0063
3	30000	191.19	285.54	0.0060	0.0060
4	35000	216.28	326.51	0.0058	0.0058

5	40000	240.67	366.65	0.0056	0.0056

Thermal Performances

HT in the shell side (annulus) and tube, Nussselt number, Reynolds number etc were calculated from the expression result in ANSYS fluent. The boundary condition in ANSYS fluent for pressure was such that the pressure drop is the inlet pressure for both shell and tube because the outlet pressure for bother are zero [15].

The velocity streamlines in the annulus sides for rectangular and triangular tube ribs are shown below in FIGURE 4. The pattern of the lines shown that the flow area of shell (annulus) is small compare to simple DPHE while the flow area in the tube is more than that of simple DPHE. The introduction of ribs has produced significant effect in flow configuration which led to heat transfer enhancement even the same length of DPHE.

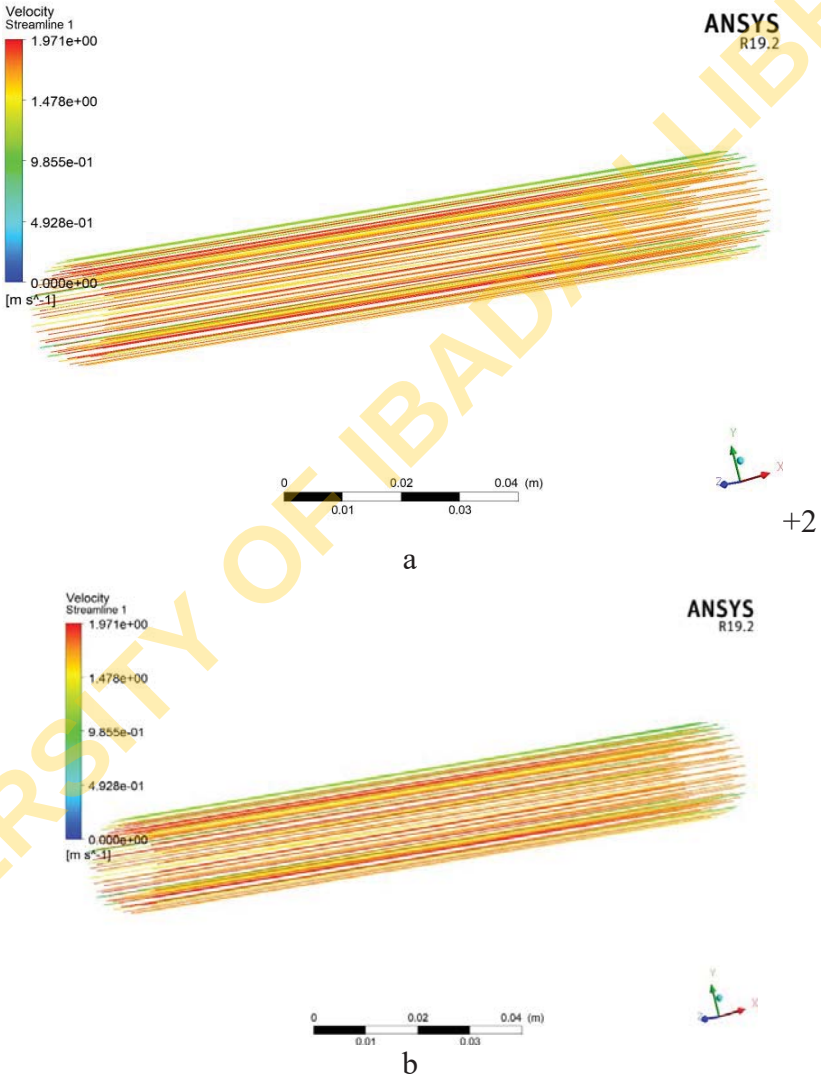

FIGURE 4. (a). Velocity streamline of DPHE with rectangle rib (annulus side)

(b) Velocity streamline of DPHE with triangle rib (annulus side).

Thermal Performance Factor (TPF) (η)

The heat transfer in the simple DPHE, DPHE with triangle rib and DPHE with rectangle rib in the annulus side were compared as shown in FIGURE 5.the graph shown that HT is increasing along with the Reynolds number and velocity. **η** for triangle rib is 29.26%, 31.76%, 32.33, 32.96%, and 33.21%, for a Reynolds number of 20000, 25000, 30000, 35000 and 40000 respectively and 30.73%, 29.57% 27.66%, 28.67%, 44.89 for rectangle rib. Therefore, increase bust thermal enhancement on the annulus side. Temperature contours in YZ plain of tube and annulus are shown in Figure 6.

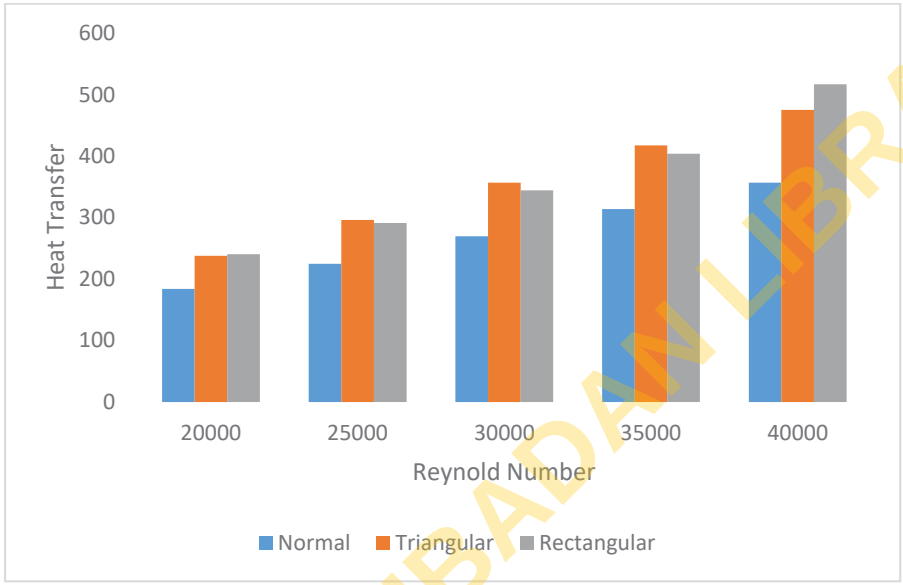

a

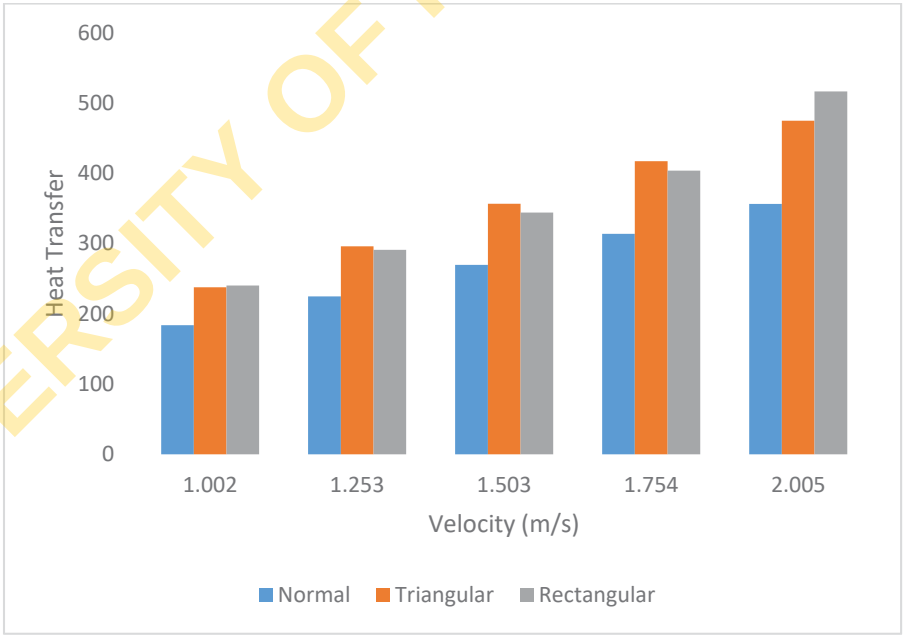

b

FIGURE 5. (a) Comparison of heat transfer in annulus side.

(b) Comparison of heat transfer in annulus side.

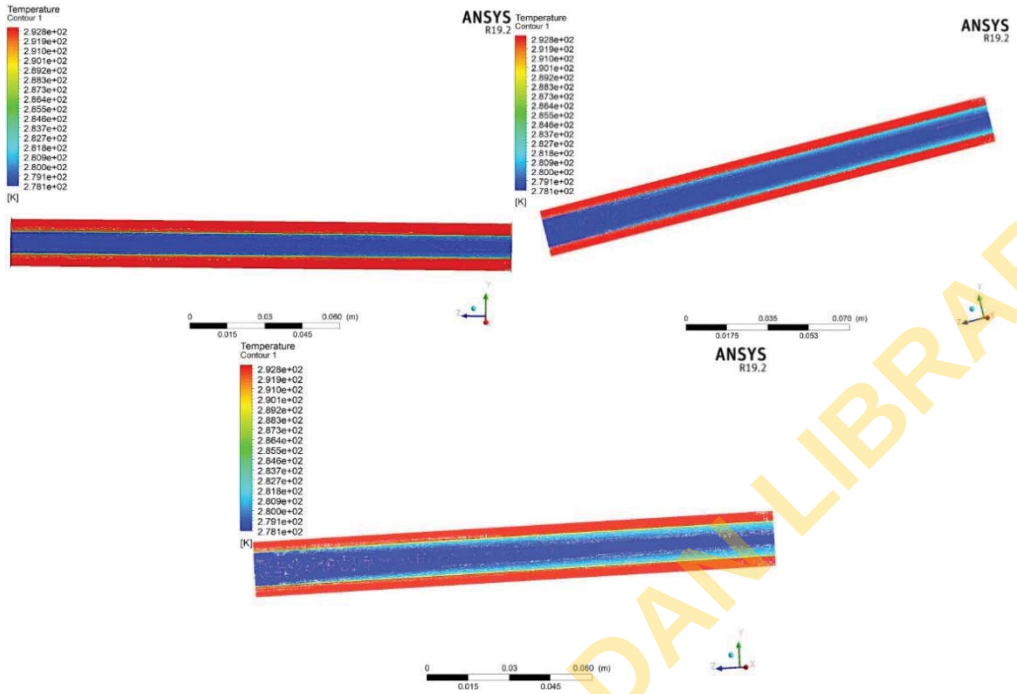

FIGURE 6. Temperature contour of DPHE

The relationship between Reynolds number and Nusselt number is shown in FIGURE 7 below. The graph shown that the increase in Re led to increase in Nu for both triangle rib and rectangle rib.

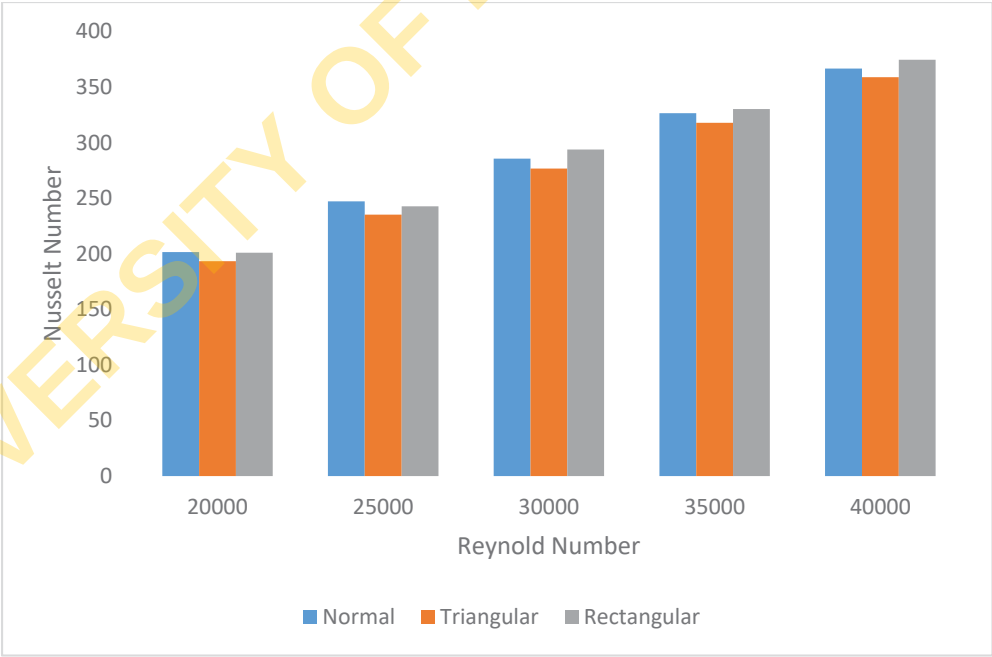

FIGURE 7. Comparison of Nusselt number of DPHE

TPF (η) can be define as the ratio of Nu number ratio (Nu_n/Nu) and the ratio of cube root of friction factor $\{(f_n/f)^{\wedge 0.33}\}$ [6]. Thermal performance and fluid dynamic performance of simple DPHE was compared with the thermal and fluid-dynamic performances of new geometric DPHE to check any improvement in heat transfer rate or thermal

performance [1]. New geometry of DPHE showed a better performance in their thermal energy movement within the device. FIGURE 8 depicts variation in TPF at different Reynolds number. TPF varied in the range of 0.9592, 0.09520, 0.9689, 0.9735 and 0.9786 for triangle rib and 0.9927, 0.9820, 1.0290, 1.0111 and 1.0214 for rectangle.

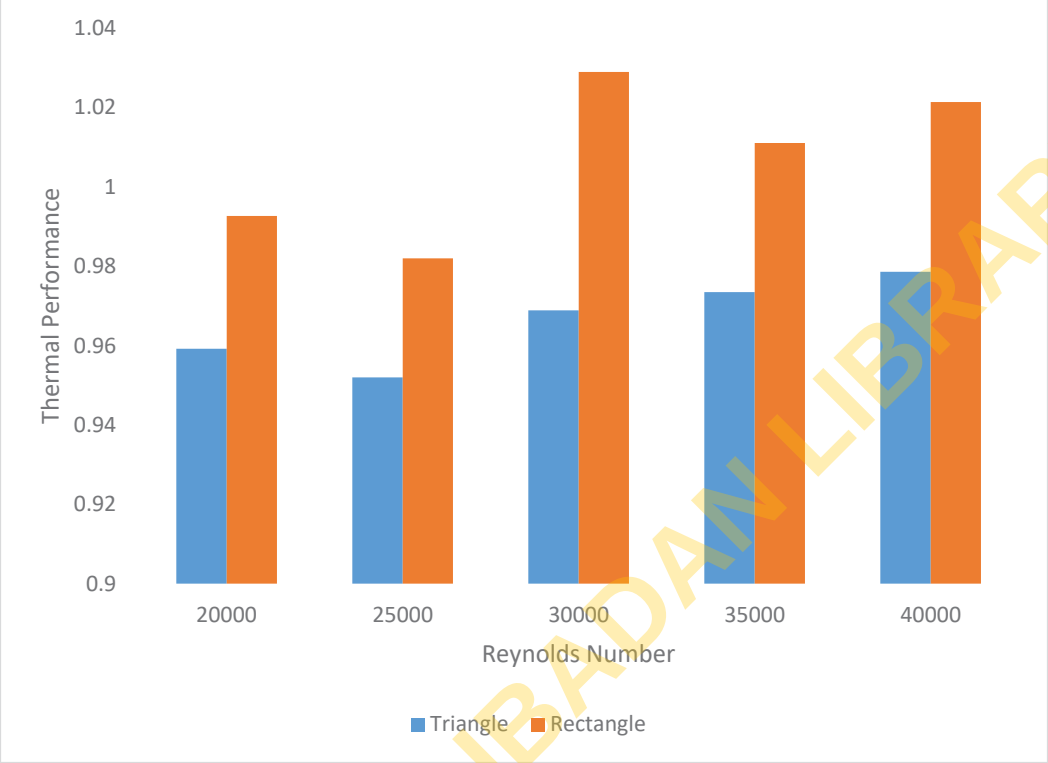

FIGURE 8. Thermal performance factor.

CONCLUSION

The new geometry has advanced the rate of HT in DPHE with the help of CFD (ANSYS fluent). ANSYS fluent is used to determine the thermo-hydraulic behaviour of DPHE with the introduction of triangle rib and rectangle rib tube. The HT is increase due to ribs. The outputs of this study show that heat transfer is enhance by 33% with the use of triangle rib and 45% with the use of rectangle rib. Triangle rib showed the highest thermal performance of 0.9786 and rectangle is 1.0290. It can be concluded that rectangle ribbed heat exchanger has better performance compare to triangle rib. However, thermal performance factor of DPHE with rectangle rib form a sine curve and this shows that for every two or three consecutive increase in Reynolds number or speed there will be a peak value of thermal performance factor which is not always correspond to the highest Reynolds number or speed of flow. Therefore, further study can be done on it for fine out the physics behind it.

ACKNOWLEDGEMENTS

The authors acknowledge Covenant University Management for the research support received from CUCRID, Covenant University, Ota.

REFERENCES

1. Akbar, A., Arani, A., & Moradi, R. (2019). *Shell and tube heat exchanger optimization using new ba ffl e and tube con fi guration*. *157*(January). https://doi.org/10.1016/j.applthermaleng.2019.113736
2. Ali, M. A., El-maghlany, W. M., Eldrainy, Y. A., & Attia, A. (2018). Heat transfer enhancement of double pipe heat exchanger using rotating of variable eccentricity inner pipe. *Alexandria Engineering Journal*. https://doi.org/10.1016/j.aej.2018.03.003

3. Ali, M. Z., Krishna, M., Reddy, D. B., & Ali, R. S. M. (2015). *Thermal Analysis of Double Pipe Heat Exchanger by Changing the Materials Using CFD*. *26*(2), 95–102.
4. Bashtani, I., & Esfahani, J. A. (2019). *ε -NTU analysis of turbulent fl ow in a corrugated double pipe heat exchanger : A numerical investigation*. *159*(June), 1–11. https://doi.org/10.1016/j.applthermaleng.2019.113886
5. Boda, M. (2017). *Design and Development of Parallel - Counter Flow Heat Exchanger*. *March*.
6. Chaurasia, S. R., & Sarviya, R. M. (2019a). Experimental thermal performance analysis of fluid flow in a heat exchanger pipe with novel double strip helical screw tape inserts for utilization of energy resources. *Energy Sources, Part A: Recovery, Utilization, and Environmental Effects*, *00*(00), 1–14. https://doi.org/10.1080/15567036.2019.1669741
7. Chaurasia, S. R., & Sarviya, R. M. (2019b). Thermal Performance Analysis of CuO/water Nanofluid Flow in a Pipe with Single and Double Strip Helical Screw Tape. *Applied Thermal Engineering*, 114631. https://doi.org/10.1016/j.applthermaleng.2019.114631
8. Chen, X., Sun, C., Xia, X., Liu, R., & Wang, F. (2019). Conjugated heat transfer analysis of a foam filled double-pipe heat exchanger for high-temperature application. *International Journal of Heat and Mass Transfer*, *134*, 1003–1013. https://doi.org/10.1016/j.ijheatmasstransfer.2019.01.100
9. El, A., Feddi, K., Saadeddine, S., Ben, A., & El, M. (2020). Performance enhancement of fi nned annulus using surface interruptions in double-pipe heat exchangers. *Energy Conversion and Management*, *210*(November 2019), 112710. https://doi.org/10.1016/j.enconman.2020.112710
10. l, A., Laknizi, A., Saadeddine, S., Ben, A., Meziane, M., & El, M. (2017). Numerical design and investigation of heat transfer enhancement and performance for an annulus with continuous helical baffles in a double-pipe heat exchanger. *Energy Conversion and Management*, *133*, 76–86. https://doi.org/10.1016/j.enconman.2016.12.002
11. Goodarzi, M., Kherbeet, A. S., Afrand, M., Sadeghinezhad, E., & Mehrali, M. (2016). Investigation of heat transfer performance and friction factor of a counter- flow double-pipe heat exchanger using nitrogen-doped , graphene-based nano fluids ☆. *International Communications in Heat and Mass Transfer*, *76*, 16–23. https://doi.org/10.1016/j.icheatmasstransfer.2016.05.018
12. Höschel, K., & Lakshminarayanan, V. (2019). Genetic algorithms for lens design: a review. *Journal of Optics (India)*, *48*(1), 134–144. https://doi.org/10.1007/s12596-018-0497-3
13. Hu, X., Sun, Q., Li, G., & Bai, S. (2019). Numerical investigation of thermo-hydraulic performance of an opposed piston opposed cylinder engine water jacket with helical fi ns. *Applied Thermal Engineering*, *159*(May), 113824. https://doi.org/10.1016/j.applthermaleng.2019.113824
14. Khan, S., & Malvi, D. (2019). *Double pipe heat exchanger with spiral flow*. 46–49.
15. Khosravi, A., Campos, H., Malekan, M., Nunes, R. O., Assad, M. E. H., Machado, L., & Pabon, J. J. G. (2019). Performance improvement of a double pipe heat exchanger proposed in a small-scale CAES system : An innovative design. *Applied Thermal Engineering*, *162*(May), 114315. https://doi.org/10.1016/j.applthermaleng.2019.114315
16. Kumar, N. T. R., Bhramara, P., Kirubeil, A., Sundar, L. S., Singh, M. K., & Sousa, A. C. M. (2018). *E ff ect of twisted tape inserts on heat transfer , friction factor of Fe 3 O 4 nano fl uids fl ow in a double pipe U-bend heat exchanger*. *c*, 53–62. https://doi.org/10.1016/j.icheatmasstransfer.2018.03.020
17. Kumar, N. T. R., Bhramara, P., Mulat, B., Sundar, L. S., Singh, M. K., & Sousa, A. C. M. (2017). Heat transfer , friction factor and effectiveness analysis of Fe 3 O 4 / water nano fl uid fl ow in a double pipe heat exchanger with return bend. *International Communications in Heat and Mass Transfer*, *81*, 155–163. https://doi.org/10.1016/j.icheatmasstransfer.2016.12.019
18. Liu, Z., Li, Y., & Zhou, K. (2016). Thermal analysis of double-pipe heat exchanger in thermodynamic vent system. *Energy Conversion and Management*, *126*, 837–849. https://doi.org/10.1016/j.enconman.2016.08.065
19. Maddah, H., Aghayari, R., Mirzaee, M., & Hossein, M. (2018). Factorial experimental design for the thermal performance of a double pipe heat exchanger using Al2O 3 -TiO 2 hybrid nano fl uid. *International Communications in Heat and Mass Transfer*, *97*, 92–102. https://doi.org/10.1016/j.icheatmasstransfer.2018.07.002
20. Majidi, D., Alighardashi, H., & Farhadi, F. (2018). Experimental studies of heat transfer of air in a double-pipe helical heat exchanger. *Applied Thermal Engineering*, *133*(January), 276–282. https://doi.org/10.1016/j.applthermaleng.2018.01.057
21. Malekan, M., Khosravi, A., & Zhao, X. (2019). The in fl uence of magnetic fi eld on heat transfer of magnetic nano fl uid in a double pipe heat exchanger proposed in a small-scale CAES system. *Applied Thermal Engineering*, *146*(August 2018), 146–159. https://doi.org/10.1016/j.applthermaleng.2018.09.117

22. Manikandan, S. (2016). *International Research Journal of Engineering and Technology (IRJET) Heat Transfer Characteristics using TiO 2 -Water Nano Fluid in Double Pipe Heat Exchanger International Research Journal of Engineering and Technology (IRJET)*. 2900–2906.
23. Mule, B. A., Hatkar, P. D. N., & Bembde, P. M. S. (2017). *ANALYSIS OF DOUBLE PIPE HEAT EXCHANGER WITH HELICAL FINS*. 961–966.
24. Omidi, M., Farhadi, M., & Jafari, M. (2017). A comprehensive review on double pipe heat exchangers. *Applied Thermal Engineering*, *110*, 1075–1090. https://doi.org/10.1016/j.applthermaleng.2016.09.027
25. Rafae, O., Mohammad, O., & Mohammed, B. (2020). *International Journal of Heat and Mass Transfer Analysis of two-phase flow in a double-pipe heat exchanger filled with porous media*. *156*. https://doi.org/10.1016/j.ijheatmasstransfer.2020.119799
26. Salem, M. R., Althafeeri, M. K., Elshazly, K. M., Higazy, M. G., & Abdrabbo, M. F. (2017). International Journal of Thermal Sciences Experimental investigation on the thermal performance of a double pipe heat exchanger with segmental perforated baf fl es. *International Journal of Thermal Sciences*, *122*, 39–52. https://doi.org/10.1016/j.ijthermalsci.2017.08.008
27. Sampson, I. E. (2020). *Design and Operation of Double Pipe Heat Exchanger*. *March 2017*.
28. Setareh, M., Sa, M., & Abdullah, A. (2019). *Experimental and numerical study on heat transfer enhancement using ultrasonic vibration in a double-pipe heat exchanger*. *159*(April). https://doi.org/10.1016/j.applthermaleng.2019.113867
29. Shahab, S., Kourosh, M., & Omid, J. (2020). Numerical simulation of nanofluid turbulent flow in a double - pipe heat exchanger equipped with circular fins. *Journal of Thermal Analysis and Calorimetry*. https://doi.org/10.1007/s10973-020-09364-w
30. Shirvan, K. M., Mirzakhanlari, S., Kalogirou, S. A., Oztop, H. F., & Mamourian, M. (2017). *International Journal of Thermal Sciences Heat transfer and sensitivity analysis in a double pipe heat exchanger fi lled with porous medium*. *121*, 124–137. https://doi.org/10.1016/j.ijthermalsci.2017.07.008
31. Sundar, L. S., Kumar, N. T. R., Mulat, B., Bhramara, P., Singh, M. K., & Sousa, A. C. M. (2019). International Journal of Heat and Mass Transfer Heat transfer and effectiveness experimentally-based analysis of wire coil with core-rod inserted in Fe 3 O 4 / water nanofluid flow in a double pipe U-bend heat exchanger. *International Journal of Heat and Mass Transfer*, *134*, 405–419. https://doi.org/10.1016/j.ijheatmasstransfer.2019.01.041
32. Tri, A., Yaningsih, I., Aziz, M., & Miyazaki, T. (2018). Double-sided delta-wing tape inserts to enhance convective heat transfer and fl uid fl ow characteristics of a double-pipe heat exchanger. *Applied Thermal Engineering*, *145*(August), 27–37. https://doi.org/10.1016/j.applthermaleng.2018.09.009
33. Wang, Q., Song, Z., Zheng, Y., Yin, Y., Liu, L., & Wang, H. (2019). Coupled convection heat transfer of water in a double pipe heat exchanger at supercritical pressures : An experimental research. *Applied Thermal Engineering*, *159*(June), 113962. https://doi.org/10.1016/j.applthermaleng.2019.113962
34. Wang, W., Zhang, Y., Lee, K., & Li, B. (2019). International Journal of Heat and Mass Transfer Optimal design of a double pipe heat exchanger based on the outward helically corrugated tube. *International Journal of Heat and Mass Transfer*, *135*, 706–716. https://doi.org/10.1016/j.ijheatmasstransfer.2019.01.115
35. Zare, K. B., Kanchan, M. D., & Patel, M. N. (n.d.). *DESIGN OF DOUBLE PIPE HEAT EXCHANGER*. 161–174.
36. Zhang, S., Lu, L., Dong, C., Hyun, S., Services, B., Hong, T., Polytechnic, K., Hom, H., & Kong, H. (2019). Thermal characteristics of perforated self-rotating twisted tapes in a double- pipe heat exchanger. *Applied Thermal Engineering*, *162*(August), 114296. https://doi.org/10.1016/j.applthermaleng.2019.114296
37. Adekeye,T, I. K. Adegun, P. O. Okekunle, A. K. Hussein, **S. O. Oyedepo**, E. Adetiba, and O.S. I. Fayomi (2017), 'Numerical Analysis of the Effects of Selected Geometrical Parameters and Fluid Properties on MHD Natural Convection Flow in an Inclined Elliptic Porous Enclosure with Localized Heating', ***Heat Transfer Asian Research***, 46(3): 261– 293
38. **Oyedepo, S.O**, R.O Fagbenle, T. O Babarinde , K.M Odunfa, A.D Oyegbile, R.O Leramo, P.O Babalola, O Kilanko and Adekeye, T (2016), 'Effect of Capillary Tube Length and Refrigerant Charge on the Performance of Domestic Refrigerator with R12 and R600a', ***International Journal of Advanced Thermofluid Research***, Vol. 2, No1: 1 – 13
39. Adebayo, J..K, A. T. Layeni, C. N. Nwaokocha**, S. O. Oyedepo** and S. O. Folarin (2019), Design and Fabrication of a Vertical Axis Wind Turbine with introduction of Plastic Gear, 3rd International Conference on Engineering for Sustainable World, Journal of Physics: Conference Series IOP Publishing, 1378 (2019) 042098, doi:10.1088/1742-6596/1378/4/042098